Bioorganic & Medicinal Chemistry Letters 25 (2015) 2314–2320

Contents lists available at ScienceDirect

Bioorganic & Medicinal Chemistry Letters

journal homepage: www.elsevier.com/locate/bmcl

# Synthesis and QSAR study of novel anti-inflammatory active mesalazine–metronidazole conjugates

Roman N. Naumov [a], Siva S. Panda [a,*], Adel S. Girgis [b], Riham F. George [c], Michel Farhat [a], Alan R. Katritzky [a,d,†]

[a] Center for Heterocyclic Compounds, Department of Chemistry, University of Florida, Gainesville, FL 32611-7200, United States
[b] Pesticide Chemistry Department, National Research Centre, Dokki, Giza 12622, Egypt
[c] Pharmaceutical Chemistry Department, Faculty of Pharmacy, Cairo University, Cairo, Egypt
[d] Chemistry Department, King Abdulaziz University, Jeddah 21589, Saudi Arabia

ARTICLE INFO

*Article history:*
Received 15 March 2015
Revised 1 April 2015
Accepted 8 April 2015
Available online 13 April 2015

*Keywords:*
Mesalazine
Metronidazole
Conjugates
Amino acids
Anti-inflammatory
QSAR

ABSTRACT

Novel, mesalazine, metronidazole conjugates **6a**–**e** with amino acid linkers were synthesized utilizing benzotriazole chemistry. Biological data acquired for all the novel bis-conjugates showed (a) some bis-conjugates exhibit comparable anti-inflammatory activity with parent drugs and (b) the potent bis-conjugates show no visible stomach lesions. 3D-pharmacophore and 2D-QSAR modeling support the observed bio-properties.



Inflammation is a protective mechanism employed by tissues against endogenous and exogenous antigens, induced by microbial infection or tissue injury and is characterized by redness, edema, fever, pain, and loss of function. Inflammation is increasingly found to be involved in the development of several chronic diseases such as arteriosclerosis, obesity, diabetes, neurodegenerative diseases and even cancer.[1,2] Non-steroidal anti-inflammatory drugs (NSAIDs) are used widely for the treatment of inflammatory and painful conditions including rheumatoid arthritis, soft tissue lesions, fever and respiratory tract infections.[3,4] The anti-inflammatory activity of NSAIDs results from enzymatic inhibition of cyclooxygenase (COX) mediated production of pro-inflammatory prostaglandins and thromboxanes.[5] COX enzymes exist in three isoforms: COX-1, COX-2, and COX-3.[6,7] The COX-1 is a constitutive enzyme found in most cells and has important roles in the protection of gastric mucosa, platelet aggregation, and renal blood flow. The COX-2 is an inducible isozyme; significantly expressed during inflammation, pain, and oncogenesis,[7] while COX-3, a splice variant of COX-1, is considered as another target for anti-inflammatory drugs.[6–8] Traditional NSAIDs interact with both (COX-1 and COX-2) and therefore their long term administration often causes gastrointestinal,[9,10] renal,[11,12] and hepatic[13] side effects. These findings have led to hypothesis that selective COX-2 inhibitors might provide good anti-inflammatory agents with improved therapeutic potency and reduced side effects. For this reason, synthesis of selective COX-2 inhibitor drugs has attracted interest in recent years in order to achieve the same anti-inflammatory activity as traditional NSAIDs but with minimal risk of undesirable gastrointestinal side effects.[14] Many selective COX-2 inhibitors such as celecoxib,[15] rofecoxib,[16] valdecoxib,[17] and etoricoxib[18] are marketed as new generation NSAIDs. However, several cardiovascular adverse effects associated with coxibs, have been reported.[19,20] Thus, novel anti-inflammatory active agents with enhanced potency and improved safety profile are still needed.

The present study describes synthesis of novel mesalazine–metronidazole conjugates and the rationale for this combination is as follows. Mesalazine '5-aminosalicylic acid, 5-ASA' is an anti-inflammatory drug used to treat inflammatory bowel disease, such as ulcerative colitis and mild-to-moderate Crohn's disease. It is used for long term maintenance therapy to prevent relapses of inflammatory bowel disease. Its oral administration however results in extensive and rapid absorption from the upper gastrointestinal tract before it reaches the colon leading to low drug bioavailability and efficiency with significant systemic side

* Corresponding author. Tel.: +1 352 870 9288; fax: +1 352 392 9199.
*E-mail address:* sspanda12@gmail.com (S.S. Panda).
† Deceased on February 10, 2014.

http://dx.doi.org/10.1016/j.bmcl.2015.04.023
0960-894X/

effects.[21–23] Metronidazole (Flagyl, Filmet) '2-(2-methyl-5-nitro-1*H*-imidazol-1-yl)ethanol' is an effective drug that possesses strong inhibitory efficacies against Gram-negative anaerobic bacteria like *Helicobacter pylori* and protozoa such as *Giardia*, *Lamblia* and *Entomoeba histolytica*.[24–26] *E. histolytica* primarily lives in the colon as a harmless commensally, but is capable of causing devastating dysentery, colitis and liver abscess.[27–29] More than 50 million people are estimated to suffer from symptoms of amoebiasis such as hemorrhagic colitis and amoebic liver abscess resulting in 100,000 deaths annually.[30] Prolonged treatment or high doses of metronidazole often cause side effects such as headache, dry mouth, metallic taste, glossitis and urticarial.[31,32] Potential carcinogenic, teratogenic, embryogenic effects and clinical and laboratory generated drug-resistance have been also described.[33]

Herein we report the synthesis of metronidazole conjugates with 5-ASA and amino acids, in order to optimize bio-active agents with enhanced pharmacological potency and safer side effects. The versatility of benzotriazole methodology allows simple preparative techniques to create complex conjugates and serves as a basis for preparation of which building block libraries. The synthesized compounds were screened for their anti-inflammatory properties utilizing the carrageenan induced paw edema technique in rats. The ulcerogenic property of the most effective synthesized agent was also investigated. Computational studies including 3D-QSAR pharmacophoric generation and 2D-QSAR (quantitative structure–activity relationship) are also reported in the present work utilizing Discovery Studio 2.5 and Comprehensive Descriptors for Structural and Statistical Analysis (CODESSA-Pro) software. This provides an understanding of the pharmacological properties and highlights the most important structural parameters controlling bio-activity.

Two synthetic routes were chosen to the target bis-conjugates with 5-ASA and amino acids, differing in the attachment of a metronidazole fragment. Such difference may affect biological activity of the target bis-conjugates, and thus affect impact of a drug on the clinical characteristics of the disease.

In the first route *N*-Cbz-protected α-amino acids were first transformed into *N*-Cbz-protected (α-aminoacyl)benzotriazoles **1a–e** (Scheme 1) via reaction with thionyl chloride. Recently we reported synthesis of mesalazine conjugates in water under microwave irradiation.[34] The products **3a–e** can also be synthesized in DMF under the same reaction conditions in the absence of base in good yields (Table 1). This later method is helpful for the hydrophilic amino acid conjugates.

The carboxylic groups of the synthesized mesalazine conjugates **3a–e** were activated by benzotriazole in presence of thionyl chloride to yield the corresponding benzotriazoles **4a–e** in yields 42–82%.[35] The compounds **4a–e** were further coupled with metronidazole in presence of DMAP in THF under microwave irradiation to obtain the corresponding bis-conjugates (Scheme 1, Table 2).[36]

The synthesized target compounds **6a–e** were characterized by NMR, CHN/HRMS spectral data, and elemental analysis. To confirm the retention of chirality of the synthesized compounds we have also synthesized a DL-form of product **6b**. The optical rotations of all the synthesized compounds **6a–e** were determined confirming the retention of chirality.

In the second route *N*-Boc-protected (α-aminoacyl)benzotriazoles **7a–e** reacted with metronidazole to give **8a–e** (Scheme 2). Unfortunately, the coupling of unprotected amino acid-metronidazole conjugates **9a–e** with *N*-acetyl-5-ASA **2b** failed and **10a–e** were not formed. Model reactions showed that **2b** is unstable in the presence of TEA which causes elimination of benzotriazole and formation of **2a**. This reaction was also tried using other coupling reagents like DCC and CDI instead of benzotriazole methodology and we were unsuccessful.

Direct esterification of **2b** with metronidazole, in the presence of DMAP, conjugate **2c** was obtained in good yield (Scheme 3). This product with no amino acid interlink in its structure was an excellent model to reveal the importance of an amino acid in biological transformations of products **6a–e**. It has also been reported that Ac-5-ASA is therapeutically active when administered by enema to patients with ulcerative colitis.

Anti-inflammatory activity of **2a**, **2c**, **6a–e** were determined in vivo by the acute carrageenan-induced paw edema standard method in rats along with their starting precursors mesalazine (**S2**), metronidazole (**S3**) at a dose of 10 mg/kg (rat body weight) indomethacin (**S1**) mol equivalent, that was used as a reference standard.[37–43] Potency, is the % inhibition of edema for the tested compounds relative to % inhibition of edema for 'reference standard' indomethacin (**S1**) at 3 h effect. This is because the maximum edema inhibitory properties of the indomethacin (**S1**) were exhibited at this time interval. From the observed results (Table 3) it was noticed that most of the compounds exhibited promising anti-inflammatory properties. Compounds **6a**, and **6d** (potency = 93.9, 100.3, respectively) exhibit potency close to or better than the standard reference (indomethacin, **S1**). Additionally, metronidazole (**S3**) also reveals remarkable anti-inflammatory properties (potency = 99.2). The anti-inflammatory properties of **S2**, **6a**, **6b**, and **6c–e** were retained up to 24 h of drug administration, explaining that some of these analogues especially, **6d** may be an effective anti-inflammatory agent against chronic symptoms. The anti-inflammatory properties of compounds **2a**, **2c**, **6b** and **6c** were exhibited with good potency at the first hour of administration and drastically reduced by time. However, the change in anti-inflammatory properties of compounds **S2**, **S3**, **6a**, **6d**, and **6e** over till the end of the fourth hour of administration, similar to the anti-inflammatory behavior of indomethacin (**S1**).

Structure–activity relationships based on the observed anti-inflammatory results revealed that, the amino acid fragment attached to the constructed mesalazine–metronidazole conjugate is a controlling factor governing the exhibited bio-activity. Attachment of the mesalazine–metronidazole conjugate with glycinyl amino acid fragment enhances the bio-properties compared to the case of alaninyl, as exhibited in pairs **6a** and **6b** (potency = 93.9, and 60.5, respectively). However, attachment of the conjugate with a valine function seems the best choice for anti-inflammatory activating agent as exhibited in compound **6d** (potency = 100.3). Presumably due to the alkyl function type of the amino acid skeleton. Conversely the conjugate with an aryalkyl group (e.g., phenylalanine) decreases the observed potency compared to alanine as shown in **6b** and **6c** (potency = 60.5, and 47.3, respectively). Compound **6b+b′** which is a racemic mixture, exhibits higher potency (potency = 73.1) than the pure stereoisomic form '*R*-isomer', **6b** (potency = 60.5). This suggests that adoption of *S*-alanine may afford more potent bio-active agent than the *R*-isomer.

Ulcerogenic liability of the most promising prepared anti-inflammatory active mesalazine–metronidazole conjugate (**6d**, potency = 100.3) along with the anti-inflammatory potent metronidazole (**S3**, potency 99.2) was investigated utilizing the standard reported method in rats[37,39,43] at the same dosage applied for the anti-inflammatory activity bio-assay [10 mg/kg (rat body weight) indomethacin (**S1**) mol equivalent]. From the observed results (Table 4), indomethacin (**S1**) exhibits ulcer index values = 6.00. However, none of the potent anti-inflammatory active agents **S3** and **6d** causes ulcers, lesions or erosions to the rat gastric mucosa. This explains the safe behavior of these compounds in any assumed technological application and also the success of the present study's aim directed toward design and synthesis of potent anti-inflammatory active hits.

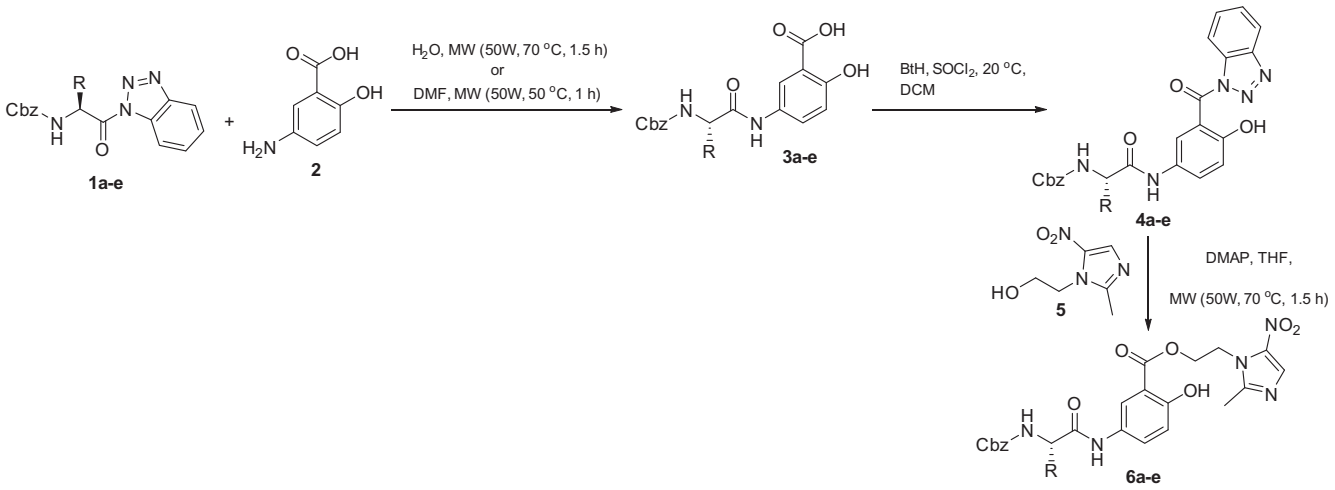


**Scheme 1.** Synthesis of amino acid–mesalazine conjugates (**6a–e**, **6b+b′**).

**Table 1**
Preparation of 5-ASA conjugates with *N*-Cbz-protected α-amino acids **3a–e** and their benzotriazole derivatives **4a–e**

| Product **3** | Yield (%), in water/DMF | Mp (°C) | Product **4** | Yield (%) | Mp (°C) |
|---|---|---|---|---|---|
| Cbz-Gly-ASA, **3a** | 68/78 | 212–214 | Cbz-Gly-ASA-Bt, **4a** | 74 | 161–163 |
| Cbz-L-Ala-ASA, **3b** | 73/70 | 236–238 | Cbz-L_Ala-ASA-Bt, **4b** | 44 | 173–175 |
| | | | Cbz-DL-Ala-ASA-Bt, **4b+b′** | 57 | 174–176 |
| Cbz-L-Phe-ASA, **3c** | 74/81 | 219–222 | Cbz-L-Phe-ASA-Bt, **4c** | 82 | 211–212 |
| Cbz-L-Val-ASA, **3d** | 76/93 | 241–243 | Cbz-L-Val-ASA-Bt, **4d** | 57 | 185–187 |
| Cbz-L-Lys(Bzl)-ASA, **3e** | 77/91 | 157–160 | Cbz-L-Lys(Bzl)-ASA-Bt, **4e** | 42 | 139–140 |

**Table 2**
Preparation of 5-ASA bis-conjugates with metronidazole and *N*-Cbz-protected α-amino acids **6a–e**

| Entry | Product **6** | Yield (%) | Mp (°C) | $[\alpha]_D^{20}$ [a] |
|---|---|---|---|---|
| 1 | Cbz-Gly-ASA-MND, **6a** | 54 | 81–83 | — |
| 2 | Cbz-L-Ala-ASA-MND, **6b** | 68 | 105–107 | −28 |
| 3 | Cbz-DL-Ala-ASA-MND, **6b+b′** | 55 | 106–108 | Racemic |
| 4 | Cbz-L-Phe-ASA-MND, **6c** | 82 | 211–212 | −31 |
| 5 | Cbz-L-Val-ASA-MND, **6d** | 57 | 185–187 | −35 |
| 6 | Cbz-L-Lys-ASA-MND, **6e** | 48 | 120–122 | −24 |

[a] *c* = 1.0, MeOH.

Toxicological behavior was studied for the most effective anti-inflammatory active analogues (**6d**, **S3**) at 50 and 100 mg/kg (mice body weight) indomethacin (**S1**) mol equivalent (i.e., 5 and 10 folds of the used anti-inflammatory dosage) utilizing the standard technique.[37,41] No dead animals or toxic symptoms were exhibited by any of the tested analogues.

The 3D-pharmacophore modeling study was performed using Discovery Studio 2.5 software (Accelrys Inc., San Diego, CA, USA) which permits 3D-pharmacophore generation, structural alignment, activity prediction and 3D-database creation.[44–47] 3D-QSAR pharmacophore protocol was used to generate predictive pharmacophores via aligning different conformations in which the molecules are likely to bind with the receptor. A given hypothesis could be combined with a known activity data to create a 3D-pharmacophore model that identifies overall aspects of molecular structure governing activity. 3D-QSAR pharmacophore was constructed using collections of molecules with activities ranging over a number of orders of magnitude. Pharmacophores explain the variability of bioactivity with respect to the geometric localization of the chemical features present in the molecules. The observed HYPOGEN identifies a 3D-array of three chemical features including two hydrogen bonding acceptors (HBA-1, HBA-2) and one negative ionizable (NegIon) (Fig. S1), which are common to the anti-inflammatory bio-active compounds **S2**, **S3**, **2a**, **2c**, **6a**, **6b** and **6c–e** that provides relative alignment for each input molecule consistent with its binding mode to a proposed common receptor site.

Pharmacophore mapping study of the synthesized anti-inflammatory active agents (Fig. S2) reveals that the most of the estimated/predicted activities (% inhibition of edema at 3 h effect) are relative to the experimentally observed values, preserving the correlated potency (Table 5). This can be attributed to the fact that the major structural factors affecting the potency of the synthesized compounds are related to their basic chemical skeleton. The highly potent anti-inflammatory active agents **6a** and **6d** show estimated activity (% inhibition of edema at 3 h effect = 40.94 and 42.75, respectively) correlated to the observed activity (% inhibition of edema at 3 h effect = 57.0 and 61.5, respectively). The mild potent anti-inflammatory active agents **6b** and **6c** exhibit similar observations (observed and estimated % inhibition of edema at 3 h effect = 37.1, 29.0; 40.75, 39.82, respectively). Slight deviation is observed for the mild anti-inflammatory active agent **6e** (observed and estimated % inhibition of edema at 3 h effect = 36.9, 41.10, respectively). The mesalazine–metronidazole conjugate which contains no amino acid function **2c** also reveals deviation regarding its bio-properties (observed and estimated % inhibition of edema at 3 h effect = 16.6, 39.98, respectively).

Mapping of the 3D-pharmacophore with the most potent anti-inflammatory active synthesized analogue **6d** exhibits the alignment of the carbonyl salicylate and the imidazoyl *N*-3 with the hydrogen bonding acceptors features HBA-1 and HBA-2, respectively while, the hydroxyl salicylate is aligned with the negative ionizable (NegIon) feature (Fig. S2). Compound **6a** which is also considered a high potent anti-inflammatory active agent exhibits a relatively different alignment compared with the highly effective analogue **6d**, where the salicylate hydroxyl and the nitro groups

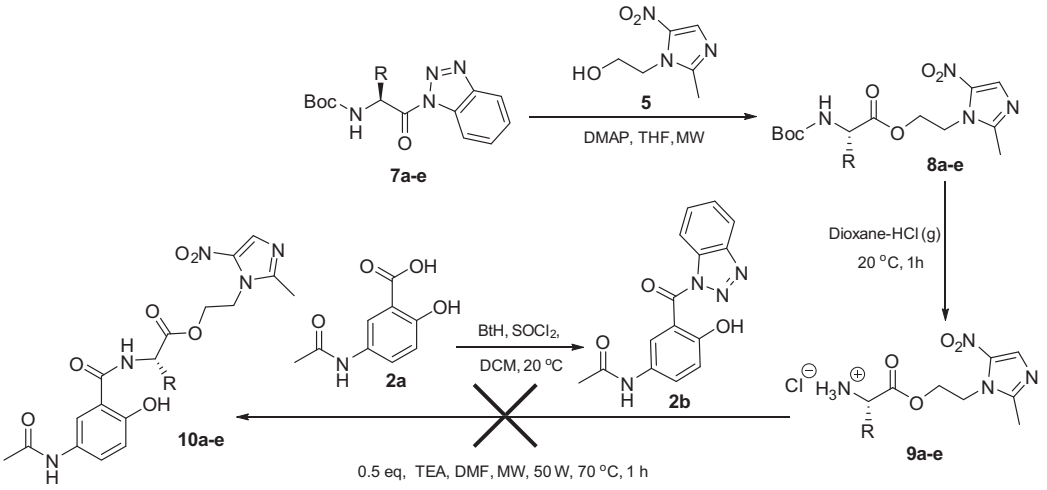


**Scheme 2.** Synthetic route toward *N*-acetylmesalazine amino acid metronidazole conjugates **10a**–**e**.

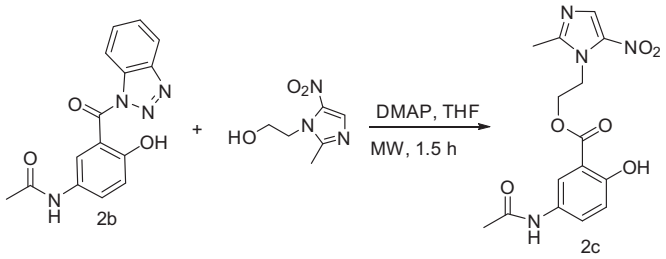


**Scheme 3.** Synthesis of *N*-acetylmesalazine metronidazole conjugate **2b**.

are aligned with the HBA-1 and HBA-2, respectively while, the carbonyl salicylate is aligned with the NegIon feature. Compounds **6b**, and **6c** (mild anti-inflammatory active agents) reveal alignment of the salicylate hydroxyl and the imidazoyl *N*-3 groups with the HBA-1 and HBA-2, respectively while, the carbonyl salicylate is aligned with the NegIon feature. A completely different alignment was viewed by compound **6e** where the (benzyloxy)carbonyl residues of the amino acid function are responsible for HBA-1 and HBA-2. This observation explains the estimated bio-activity properties of compound **6e** relative to its experimentally observed activity. Additionally, the alignment observations support the attained SAR rules mentioned previously for example, the highly potent analogue **6d** due to its iso-propyl residue (+I effect) of valine amino acid strengthen alignment of both carbonyl and hydroxyl salicylate in HBA-1 and NegIon functions, respectively. Potency difference between compounds **6d** and **6b** which was attributed to the amino acid fragment difference in SAR is also supported herein. Although compound **6b** exhibits a slight alignment division than **6d**, the carbonyl and hydroxyl salicylate are aligned with NegIon and HBA-1 functions. Thus, the potency difference can be attributed to the alkyl function of amino acid fragment (+I effect of methyl is less than that of *iso*-propyl) which mainly responsible for alignment efficiency.

2D-QSAR was undertaken utilizing CODESSA-Pro software. The basic idea behind QSAR is to generate a relationship between the chemical structure of an organic compound and its physico-chemical properties. Due to the limited pharmacologically active data set mentioned in the present study, external data points were considered. The external data points are derived from anti-inflammatory active agents determined by the same standard technique adopted in the present study (in vivo acute carrageenan-induced paw edema technique in rats at a dose of 10 mg/kg 'rat body weight' indomethacin, **S1** mol equivalent).[37] The QSAR study was undertaken using comprehensive descriptors for structural and statistical analysis (CODESSA-Pro) software employing the synthesized compounds of the present study **S1**–**S3**, **2a**, **2c**, **6a**–**e** in addition to 14 compounds which are reported by our group[37] forming a total of 24 compounds used as a training set for constructing a reliable QSAR model (Table 6).

Geometry of the training set compounds was optimized using molecular mechanics force field ($MM^+$) followed by the

**Table 3**
Bio-assay results for the tested compounds at 10 mg/kg (rat body weight) indomethacin (**S1**) mol equivalent

| Entry | Compd | Mean edema thickness 'mm' (% inhibition of edema) | | | | | Potency* |
|---|---|---|---|---|---|---|---|
| | | 1 h | 2 h | 3 h | 4 h | 24 h | |
| 1 | Control | 1.283 ± 0.052 (00.0) | 1.395 ± 0.003 (00.0) | 1.588 ± 0.036 (00.0) | 1.748 ± 0.058 (00.0) | 0.993 ± 0.011 (00.0) | – |
| 2 | **S1** (indomethacin) | 0.663 ± 0.068 (48.3) | 0.624 ± 0.093 (55.3) | 0.615 ± 0.092 (61.3) | 0.734 ± 0.092 (58.0) | 0.993 ± 0.093 (00.0) | 100.0 |
| 3 | **S2** (mesalazine) | 0.465 ± 0.043 (63.8) | 0.653 ± 0.087 (53.2) | 0.675 ± 0.008 (57.5) | 0.833 ± 0.053 (52.3) | 0.610 ± 0.023 (38.6) | 93.8 |
| 4 | **S3** (metronidazole) | 0.433 ± 0.008 (66.3) | 0.470 ± 0.001 (66.3) | 0.622 ± 0.010 (60.8) | 0.718 ± 0.066 (58.9) | 0.993 ± 0.020 (00.0) | 99.2 |
| 5 | **6a** | 0.563 ± 0.011 (56.1) | 0.607 ± 0.082 (56.5) | 0.683 ± 0.060 (57.0) | 0.825 ± 0.097 (52.8) | 0.823 ± 0.011 (17.1) | 93.9 |
| 6 | **6b** | 0.533 ± 0.054 (58.5) | 0.872 ± 0.062 (37.5) | 0.999 ± 0.044 (37.1) | 1.117 ± 0.089 (36.1) | 0.878 ± 0.064 (11.6) | 60.5 |
| 7 | **6b+b′** | 0.540 ± 0.088 (57.9) | 0.740 ± 0.082 (47.0) | 0.877 ± 0.002 (44.8) | 1.030 ± 0.041 (41.1) | 0.993 ± 0.098 (00.0) | 73.1 |
| 8 | **6c** | 0.580 ± 0.070 (54.8) | 0.975 ± 0.047 (30.1) | 1.127 ± 0.025 (29.0) | 1.267 ± 0.008 (27.5) | 0.663 ± 0.054 (33.2) | 47.3 |
| 9 | **6d** | 0.328 ± 0.015 (74.4) | 0.495 ± 0.054 (64.5) | 0.611 ± 0.052 (61.5) | 0.730 ± 0.077 (58.2) | 0.480 ± 0.066 (51.7) | 100.3 |
| 10 | **6e** | 0.715 ± 0.024 (44.3) | 0.868 ± 0.092 (37.8) | 1.002 ± 0.052 (36.9) | 1.163 ± 0.055 (33.5) | 0.761 ± 0.007 (23.4) | 60.2 |
| 11 | **2a** | 0.728 ± 0.055 (43.3) | 1.285 ± 0.051 (7.9) | 1.568 ± 0.007 (1.3) | 1.748 ± 0.072 (00.0) | 0.993 ± 0.009 (00.0) | 2.1 |
| 12 | **2c** | 0.470 ± 0.008 (63.4) | 1.053 ± 0.064 (24.5) | 1.324 ± 0.091 (16.6) | 1.477 ± 0.047 (15.5) | 0.993 ± 0.096 (00.0) | 27.1 |

* Potency was expressed as % inhibition of edema for the tested compounds relative to % inhibition of edema for indomethacin 'reference standard' (**S1**) at 3 h effect.

**Table 4**
Ulcerogenic liability of the most promising anti-inflammatory active agents

| Compd | Number of animals with ulcer | % incidence of ulcer divided by 10 | Average of ulcer number | Average severity of ulcer | Ulcer index |
|---|---|---|---|---|---|
| Control | 0/6 | 0 | 0 | 0 | 0 |
| **S1** (indomethacin) | 3/6 | 5.00 | 0.50 | 0.50 | 6.00 |
| **S3** (metronidazole) | 0/6 | 0 | 0 | 0 | 0 |
| **6d** | 0/6 | 0 | 0 | 0 | 0 |

**Table 5**
Best fit values and estimated/predicted activities (% inhibition of edema at 3 h effect) for the anti-inflammatory active synthesized compounds **S2, S3, 2a, 2c, 6a, 6b** and **6c–e** mapped with the generated 3D-pharmacophore model

| Entry | Compd | Observed % inhibition of edema | Estimated % inhibition of edema | Fit value |
|---|---|---|---|---|
| 1 | **S2** | 57.5 | 40.00 | 3.823 |
| 2 | **S3** | 60.8 | 50.65 | 3.720 |
| 3 | **6a** | 57.0 | 40.94 | 3.813 |
| 4 | **6b** | 37.1 | 40.75 | 3.815 |
| 5 | **6c** | 29.0 | 39.82 | 3.825 |
| 6 | **6d** | 61.5 | 42.75 | 3.794 |
| 7 | **6e** | 36.9 | 41.10 | 3.811 |
| 8 | **2a** | 1.3 | 1.13 | 5.371 |
| 9 | **2c** | 16.6 | 39.98 | 3.823 |

**Table 6**
Observed and predicated values of the tested anti-inflammatory active agents according to the multi-linear QSAR model[a]

| Entry | Compd | Observed % inhibition of edema at 3 h effect | Predicted % inhibition of edema at 3 h effect | Error |
|---|---|---|---|---|
| 1 | **S1** | 61.3 | 77.3 | −16.0 |
| 2 | **S2** | 57.5 | 46.3 | 11.2 |
| 3 | **S3** | 60.8 | 56.3 | 4.5 |
| 4 | **6a** | 57.0 | 52.5 | 4.5 |
| 5 | **6b** | 37.1 | 42.0 | −4.9 |
| 6 | **6c** | 29.0 | 17.8 | 11.2 |
| 7 | **6d** | 61.5 | 49.7 | 11.8 |
| 8 | **6e** | 36.9 | 50.9 | −14.0 |
| 9 | **2a** | 1.3 | 1.4 | −0.1 |
| 10 | **2c** | 16.6 | 20.5 | −3.9 |

[a] Activity was undertaken as % inhibition of edema for the tested compounds at 3 h effect.

semi-empirical AM1 method implemented in the HyperChem 8.0 package. The structures were fully optimized without fixing any parameters, thus bringing all geometric variables to their equilibrium values. The energy minimization protocol employed the Polake–Ribiere conjugated gradient algorithm. Convergence to a local minimum was achieved when the energy gradient was $\leqslant$0.01 kcal/mol. The RHF method was used in spin pairing for the two semi-empirical tools.[37,44,45,48,49] The resulting output files were exported to CODESSA-Pro that includes MOPAC capability for final geometry optimization. CODESSA-Pro software includes the following: (a) a calculation engine for more than 500 descriptors and (b) an engine for the development of the statistically most important linear and nonlinear QSAR regression models. CODESSA-Pro calculated 684 molecular descriptors including constitutional, topological, geometrical, charge-related, semi-empirical, thermodynamic, molecular-type, atomic-type and bond-type descriptors for the exported 24 bio-active agents. Different mathematical transformations of the experimentally observed property 'activity' [% inhibition of edema for the tested compounds at 10 mg/kg (rat body weight) indomethacin (**S1**) mol equivalent at 3 h effect], 1/property, log(property) and 1/log(property) values in searching for the best QSAR models.

Best multi-linear regression (BMLR) was utilized which is a stepwise search for the best *n*-parameter regression equations (where, *n* stands for the number of descriptors used), based on the highest $R^2$ (squared correlation coefficient), $R^2_{cv}$OO (squared cross-validation 'leave one-out, LOO' coefficient), $R^2_{cv}$MO (squared cross-validation 'leave many-out, LMO' coefficient), *F* (Fisher statistical significance criteria) values, and $s^2$ (standard deviation). The multi-parameter linear regression method establishes a correlation between the dependent variable (property) and independent variable (theoretical or experimental descriptors). The BMLR method includes finding all orthogonal pairs of descriptors in the dataset and building two-descriptor models with orthogonal pairs of descriptors previously found. Finally additional descriptors are added to the two-descriptor equations until the additional descriptors cease to bring improvement in *F*. Thereafter the stepwise procedure is stopped according to the $R^2$, $R^2_{CV}$ and *F* values until best equations obtained. The QSAR models up to 4 descriptor models describing bio-activity of the anti-inflammatory active agents were generated (obeying the thumb rule of 5:1, which is the ratio between the data points and the number of QSAR descriptor models). Statistical characteristics of the QSAR models are presented in Table 7. The established QSAR model is statistically significant. The descriptors are sorted in descending order of the respective values of the Student's *t*-criterion, which is a widely accepted measure of statistical significance of individual parameters in multiple linear regressions. Figure 1 exhibits the QSAR multi-linear model plot of correlations representing the observed versus predicted log[% inhibition of edema for the tested compounds at 10 mg/kg (rat body weight) indomethacin (**S1**) mol equivalent at 3 h effect]. The scattered plots are uniformly distributed, covering ranges, observed 0.114–1.853; predicted 0.156–1.888 logarithmic units, respectively.

Molecular descriptors are the physico-chemical parameters used to correlate chemical structure and property value expressed as log[% inhibition of edema for the tested compounds at 10 mg/kg (rat body weight) indomethacin (**S1**) mol equivalent at 3 h effect]. The first descriptor controlling the attained QSAR model based on its *t*-criterion (9.008) is minimum total interaction for bond C–C, which is a semi-empirical descriptor used as a measure of the bond strength.[50] The second descriptor of the QSAR model ($t$ = 5.688) is FPSA-3 fractional PPSA (PPSA-3/TMSA) which is a charge-related descriptor. Fractional atomic charge weighted partial positive surface area (FPSA-3) is determined by Eq. 1.[51]

**Table 7**
Descriptor of the best multi-linear QSAR model

| ID | $N$ = 24, $n$ = 4, $R^2$ = 0.873, $R^2$cvOO = 0.796, $R^2$cvMO = 0.787, $F$ = 32.597, $s^2$ = 0.023 | | | |
|---|---|---|---|---|
| | Coefficient | *s* | *t* | Descriptor |
| 0 | −3.768 | 1.434 | −2.627 | Intercept |
| $D_1$ | 1.221 | 0.136 | 9.008 | Min. total interaction for bond C–C |
| $D_2$ | 46.370 | 8.152 | 5.688 | FPSA-3 fractional PPSA (PPSA-3/TMSA) (MOPAC PC) |
| $D_3$ | −25.707 | 2.781 | −9.245 | Relative number of O atoms |
| $D_4$ | −1.725 | 0.155 | −11.121 | Min. coulombic interaction for bond C–O |

log [% inhibition of edema for the tested compounds at 10 mg/kg (rat body weight) indomethacin (**S1**) mol equivalent at 3 h effect] = −3.768 + (1.221 × $D_1$) + (46.370 × $D_2$) − (25.707 × $D_3$) − (1.725 × $D_4$).

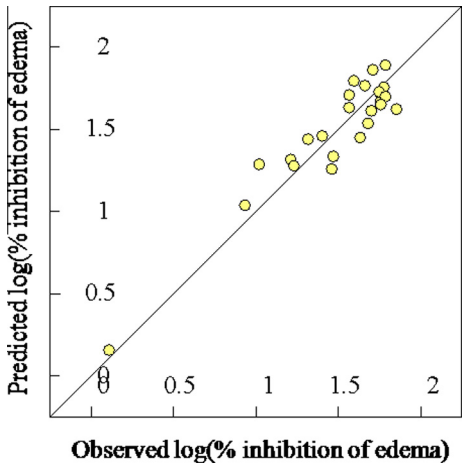


**Figure 1.** QSAR best multi-linear model plot of correlations representing the observed versus predicted log[% inhibition of edema for the tested compounds at 10 mg/kg (rat body weight) indomethacin (**S1**) mol equivalent at 3 h effect].

$$\mathrm{FNSA3} = \frac{\mathrm{PNSA3}}{\mathrm{TMSA}}. \quad (1)$$

where, PNSA3 stands for total charge weighted partial positively charged molecular surface area, and TMSA for total molecular surface area. This descriptor has the highest coefficient (46.370) among the other descriptors controlling the attained QSAR model. This observation coincide with our mentioned SAR rules as well as 3D-pharmacophoric hypothesis governing bio-activity concerning type of amino acid fragment attached to the constructed mesalazine–metronidazole conjugate. For example, the amino acid function of compound **6d** (valine), through its electron donating property (+I effect of *iso*-propyl function) facilitate the hydrogen bonding acceptor behavior of salicylate functional groups, in more efficiency than that of alanine (compound **6b**). Relative number of O atoms is the third descriptor governing the QSAR model ($t = -9.245$) is a constitutional descriptor. This descriptor has the lowest share in the QSAR model (coefficient = −25.707). In other words, the high value of this descriptor (relative number of O atoms), the low log(property, % inhibition of edema) so, the low potency of the constructed compound. The last descriptor of the QSAR model is minimum coulombic interaction for bond C–O, which is a semi-empirical descriptor.

The reliability and statistical relevance of the QSAR model is examined by internal validation procedure which seems the most appropriate statistical technique for the present study mainly due to the limited data set used (24 compounds). Internal cross validation is applied by the CODESSA-Pro technique employing both Leave One Out (LOO), which involves developing a number of models with one example omitted at a time, and Leave Many Out (LMO), which involves developing a number of models with many data points omitted at a time (up to 20% of the total data points). The observed correlations due to the internal cross validation techniques are 0.796, and 0.787 corresponding to $R^2$cvOO, and $R^2$cvMO, respectively. All of them are significantly correlated with the squared correlation coefficient of the attained QSAR model ($R^2 = 0.873$). Standard deviation of the regressions, $s^2 = 0.023$ is also a measurable value for the QSAR model together with the Fisher test value, $F = 32.597$ that reflects the ratio of the variance explained by the model and the variance due to their errors. A high value of *F*-test compared with the $s^2$ is a validation of the model.

The predicted/estimated bio-properties due to the attained QSAR model of most of the synthesized mesalazine–metronidazole conjugates are compatible to their experimental observed values preserving their relative potencies (Table 6). Compound **6a**, which is considered a highly potent anti-inflammatory active agent reveals predicted % inhibition of edema 52.5, correlated well with its observed bio-activity (% inhibition of edema = 57.0). A slight deviation was exhibited for compound **6d** (observed and predicted property = 61.5, 49.7, respectively). Good predicted bio-activity was exhibited by the QSAR model due to compounds **6b** and **6c**, which are considered mild anti-inflammatory active agents, compatible to their observed properties (observed and predicted property = 37.1, 29.0; 42.0, 17.8 for compounds **6b** and **6c**, respectively). All of these observations give good indications for the predictive power of the attained QSAR model not only for validating the observed bio-data but also for optimizing high potent hits having mesalazine–metronidazole conjugate scaffold.

In conclusion, synthesis of compounds possessing mesalazine–metronidazole conjugate scaffold can afford a promising anti-inflammatory active agent. Although the acetyl mesalazine–metronidazole conjugate **2c** reveals a mild anti-inflammatory activity (potency = 27.1), the bio-properties were enhanced greatly when an amino acid fragment was included instead of the acetyl function as exhibited in compounds **6a** and **6d** (potency = 93.9, and 100.3, respectively), which possess glycine and valine amine acid residue. SAR rules were attained due to the synthesized analogues and supported by a 3D-pharmacophore modeling possessing three features 'two hydrogen bonding acceptors and one negative ionizable'. A robust 4-describtor 2D-QSAR model was attained utilizing CODESSA-Pro software ($N = 24$, $n = 4$, $R^2 = 0.873$, $R^2$cvOO = 0.796, $R^2$cvMO = 0.787, $F = 32.597$, $s^2 = 0.023$) validating the observed anti-inflammatory bio-properties and supporting the attained controlling parameters governing bio-data.

## Acknowledgments

We thank the University of Florida, United States and the Kenan Foundation for financial support.

## Supplementary data

Supplementary data (synthetic procedure, analysis data, 3D-pharmacophore data) associated with this article can be found, in the online version, at http://dx.doi.org/10.1016/j.bmcl.2015.04.023.

## References and notes

1. Garcia-Lafuente, A.; Guillamon, E.; Villares, A.; Rostagno, M. A.; Martinez, J. A. *Inflamm. Res.* **2009**, *58*, 537.
2. Freitas, M.; Ribeiro, D.; Tom, S. M.; Silva, A. M. S.; Fernandes, E. *Eur. J. Med. Chem.* **2014**, *86*, 153.
3. Sorbera, L. A.; Lesson, P. A.; Castanar, J.; Castanar, R. M. *Drugs Future* **2001**, *26*, 133.
4. Yadav, P.; Singh, P.; Tewari, A. K. *Bioorg. Med. Chem. Lett.* **2014**, *24*, 2251.
5. Zebardast, T.; Zarghi, A.; Daraie, B.; Hedayati, M.; Dadrass, O. G. *Bioorg. Med. Chem. Lett.* **2009**, *19*, 3162.
6. Chandrasekharan, N. V.; Dai, H.; Roos, K. L.; Evanson, N. K.; Tomsik, J.; Elton, T. S.; Simmons, D. L. *PNAS* **2002**, *99*, 13926.
7. Bansal, S.; Bala, M.; Suthar, S. K.; Choudhary, S.; Bhattacharya, S.; Bhardwaj, V.; Singla, S.; Joseph, A. *Eur. J. Med. Chem.* **2014**, *80*, 167.
8. Parente, L.; Perretti, M. *Biochem. Pharmacol.* **2003**, *65*, 153.
9. Botting, R. M. *J. Therm. Biol.* **2006**, *31*, 208.
10. Naesdal, J.; Brown, K. *Drug Safety* **2006**, *29*, 119.
11. Schneider, V.; Levesque, L. E.; Zhang, B.; Hutchinson, T.; Brophy, J. M. *Am. J. Epidemiol.* **2006**, *164*, 881.
12. Mounier, G.; Guy, C.; Berthoux, F.; Beyens, M. N.; Ratrema, M.; Ollagnier, M. *Therapie* **2006**, *61*, 255.
13. Adebayo, D.; Bjarnason, I. *Postgraduate Med. J.* **2006**, *82*, 186.
14. Rathish, I. G.; Javed, K.; Ahmad, S.; Bano, S.; Alam, M. S.; Pillai, K. K.; Singh, S.; Bagchi, V. *Bioorg. Med. Chem. Lett.* **2009**, *19*, 255.
15. Penning, T. D.; Talley, J. J.; Bertenshaw, S. R.; Carter, J. S.; Collins, P. W.; Docter, S.; Graneto, M. J.; Lee, L. F.; Malecha, J. W.; Miyashiro, J. M.; Rogers, R. S.; Rogier, D. J.; Yu, S. S.; Anderson, G. D.; Burton, E. G.; Cogburn, J. N.; Gregory, S. A.;

Koboldt, C. M.; Perkins, W. E.; Seibert, K.; Veenhuizen, A. W.; Zhang, Y. Y.; Isakson, P. C. *J. Med. Chem.* **1997**, *40*, 1347.
16. Prasit, P.; Wang, Z.; Brideau, C.; Chan, C. C.; Charleson, S.; Cromlish, W.; Ethier, D.; Evans, J. F.; Ford-Hutchinson, A. W.; Gauthier, J. Y. *Bioorg. Med. Chem. Lett.* **1999**, *9*, 1773.
17. Talley, J. J.; Brown, D. L.; Carter, J. S.; Graneto, M. J.; Koboldt, C. M.; Masferrer, J. L.; Perkins, W. E.; Rogers, R. S.; Shaffer, A. F.; Zhang, Y. Y.; Zweifel, B. S.; Seibert, K. *J. Med. Chem.* **2000**, *43*, 775.
18. Riendeau, D.; Percival, M. D.; Brideau, C.; Charleson, S.; Dube, D.; Ethier, D.; Falgueyret, J. P.; Friesen, R. W.; Gordon, R.; Greig, G.; Guay, J.; Mancini, J.; Ouellet, M.; Wong, E.; Xu, L.; Boyce, S.; Visco, D.; Girard, Y.; Prasit, P.; Zamboni, R.; Rodger, I. W.; Gresser, M.; Ford-Hutchinson, A. W.; Young, R. N.; Chan, C. C. *J. Pharm. Exp. Ther.* **2001**, *296*, 558.
19. Dogne, J. M.; Supuran, C. T.; Pratico, D. *J. Med. Chem.* **2005**, *48*, 2251.
20. McGettigan, P.; Henry, D. *J. Am. Med. Assoc.* **2006**, *296*, 1633.
21. Dhaneshwar, S. S.; Chail, M.; Patil, M.; Naqvi, S.; Vadnerkar, G. *Eur. J. Med. Chem.* **2009**, *44*, 131.
22. Kim, J.; Kang, S.; Hong, S.; Yum, S.; Kim, Y. M.; Jung, Y. *Eur. J. Med. Chem.* **2012**, *48*, 36.
23. Banić-Tomišić, Z.; Kojić-Prodić, B.; Širola, I. *J. Mol. Struct.* **1997**, *416*, 209.
24. Cui, S.-F.; Peng, L.-P.; Zhang, H.-Z.; Rasheed, S.; Kumar, K. V.; Zhou, C.-H. *Eur. J. Med. Chem.* **2014**, *86*, 318.
25. Sutherland, H. S.; Blaser, A.; Kmentova, I.; Franzblau, S. G.; Wan, B.; Wang, Y.; Ma, Z.; Palmer, B. D.; Denny, W. A.; Thompson, A. M. *J. Med. Chem.* **2010**, *53*, 855.
26. Zhang, L.; Chang, J.-J.; Zhang, S.-L.; Damu, G. L. V.; Geng, R.-X.; Zhou, C.-H. *Bioorg. Med. Chem.* **2013**, *21*, 4158.
27. Wani, M. Y.; Bhat, A. R.; Azam, A.; Athar, F. *Eur. J. Med. Chem.* **2013**, *64*, 190.
28. Hammami, N.; Drissi, C.; Sebai, R.; Araar, M.; Maatallah, Y.; Belghith, L.; Nagi, S.; Hentati, F.; Ben-Hamouda, M. *J. Neuroradiol.* **2007**, *34*, 133.
29. Kim, D.; Park, J.; Yoon, B.; Baek, M. J.; Kim, J. E.; Kim, S. Y. *J. Neurol. Sci.* **2004**, *224*, 107.
30. Stanley, S. L., Jr. *Lancet* **2003**, *361*, 1025.
31. Bansal, D.; Sehgal, R.; Chawla, Y.; Mahajan, R. C.; Malla, N. *Ann. Clin. Microbiol. Antimicrob.* **2004**, *3*, 27.
32. Cano, P. A.; Islas-Jácome, A.; González-Marrero, J.; Yépez-Mulia, L.; Calzada, F.; Gámez-Montaño, R. *Bioorg. Med. Chem.* **2014**, *22*, 1370.
33. Upcroft, P.; Upcroft, J. *Clin. Microbiol. Rev.* **2001**, *14*, 150.
34. Ibrahim, M. A.; Panda, S. S.; Alamry, K. A.; Katritzky, A. R. *Synthesis* **2013**, *45*, 3255.
35. *Synthesis of benzyl(2-((3-(1H-benzo[d][1,2,3]triazole-1-carbonyl)-4-hydroxyphenyl) amino)-2-oxoethyl)carbamate* (**4a**)*, representative procedure*: in a 50 mL round bottom flask equipped with a small magnetic stir bar benzotriazole (1.0 equiv) was dissolved in DCM (20 mL) under nitrogen atmosphere and thionyl chloride (1.2 equiv) was added with a syringe. The resulting solutions were allowed to be stirred for 20 min at room temperature, then **3a** was added and the reaction mixture was stirred for the next 6 h at room temperature. The solid precipitated was filtered off, washed with 4 N HCl, sodium bicarbonate and water to yield the product as yellow microcrystals. Yield: 74%; mp 161.0–163.0 °C; $^1$H NMR (DMSO-$d_6$): $\delta$ 10.10 (s, 1H), 9.99 (s, 1H), 8.27 (d, $J$ = 8.1 Hz, 2H), 7.89–7.78 (m, 2H), 7.70–7.60 (m, 2H), 7.58–7.50 (m, 1H), 7.43–7.25 (m, 5H), 6.97 (d, $J$ = 8.7 Hz, 1H), 5.04 (s, 2H), 3.79 (d, $J$ = 6.1 Hz, 1H); $^{13}$C NMR (DMSO-$d_6$): $\delta$ 167.8, 166.6, 156.6, 152.0, 145.4, 137.04, 130.8, 130.8, 130.6, 128.4, 127.8, 127.8, 126.6, 125.1, 120.8, 120.4, 120.0, 116.8, 113.9, 65.5, 44.0; HRMS $m/z$ for $C_{23}H_{19}N_5O_5$ [M+H]$^+$ calcd 446.1459, found 446.1460
36. *Synthesis of 2-(2-methyl-5-nitro-1H-imidazol-1-yl)ethyl 5-(2-(((benzyloxy) carbonyl)amino)acetamido)-2-hydroxybenzoate* (**6a**)*, representative procedure:* Cbz-protected (α-aminoacyl-5-aminosalicyl)benzotriazolide **4a** (1.0 equiv) and metronidazole (1.1 equiv) were dissolved in THF (4 mL) under nitrogen atmosphere in a dried heavy-walled Pyrex tube equipped with a small magnetic stirrer bar. Then DMAP (0.5 equiv) was added and the reaction mixtures were exposed to microwave irradiation (50 W) at 70 °C for 1.5 h. The mixture was allowed to cool through an inbuilt system until the temperature fell below 30 °C (ca. 10 min). The resulting reaction mixture was poured onto crushed ice and the solid precipitated was filtered and washed with 2 N HCl, water and ether to give the desired product as grey microcrystals. Yield 54%; mp 81.0–83.0 °C; $^1$H NMR (methanol-$d_4$): $\delta$ 8.10 (s, 1H), 8.01 (s, 1H), 7.49 (d, $J$ = 10.4 Hz, 1H), 7.45–7.23 (m, 5H), 6.90 (d, $J$ = 8.9 Hz, 1H), 5.13 (s, 2H), 4.80 (s, 4H), 3.92 (s, 2H), 2.55 (s, 3H); $^{13}$C NMR (methanol-$d_4$): $\delta$ 170.4, 170.2, 159.5, 159.2, 138.1, 132.8, 131.4, 130.2, 129.5, 129.0, 128.9, 128.9, 125.7, 122.4, 118.8, 112.5, 67.9, 64.4, 46.4, 45.3, 14.2; HRMS $m/z$ for $C_{23}H_{23}N_5O_8$ [M+H]$^+$ calcd 498.1619, found 498.1623.
37. Tiwari, A. D.; Panda, S. S.; Girgis, A. S.; Sahu, S.; George, R. F.; Srour, A. M.; La Starza, B.; Asiri, A. M.; Hall, C. D.; Katritzky, A. R. *Org. Biomol. Chem.* **2014**, *12*, 7238.
38. Girgis, A. S.; Tala, S. R.; Oliferenko, P. V.; Oliferenko, A. A.; Katritzky, A. R. *Eur. J. Med. Chem.* **2012**, *50*, 1.
39. Barsoum, F. F.; Girgis, A. S. *Eur. J. Med. Chem.* **2009**, *44*, 2172.
40. Girgis, A. S.; Barsoum, F. F. *Eur. J. Med. Chem.* **2009**, *44*, 1972.
41. Girgis, A. S.; Mishriky, N.; Ellithey, M.; Hosni, H. M.; Farag, H. *Bioorg. Med. Chem.* **2007**, *15*, 2403.
42. Girgis, A. S.; Ellithey, M. *Bioorg. Med. Chem.* **2006**, *14*, 8527.
43. Barsoum, F. F.; Hosni, H. M.; Girgis, A. S. *Bioorg. Med. Chem.* **2006**, *14*, 3929.
44. Girgis, A. S.; Stawinski, J.; Ismail, N. S. M.; Farag, H. *Eur. J. Med. Chem.* **2012**, *47*, 312.
45. Girgis, A. S.; Farag, H.; Ismail, N. S. M.; George, R. F. *Eur. J. Med. Chem.* **2011**, *46*, 4964.
46. Girgis, A. S.; Ismail, N. S. M.; Farag, H. *Eur. J. Med. Chem.* **2011**, *46*, 2397.
47. Girgis, A. S.; Ismail, N. S. M.; Farag, H.; El-Eraky, W. I.; Saleh, D. O.; Tala, S. R.; Katritzky, A. R. *Eur. J. Med. Chem.* **2010**, *45*, 4229.
48. Ahmed Farag, I. S.; Girgis, A. S.; Moustafa, A. M.; El-Gendy, B. E. M.; Mabied, A. F.; Shalaby, E. M. *J. Mol. Struct.* **2014**, *1075*, 327.
49. Girgis, A. S.; Panda, S. S.; Ahmed Farag, I. S.; El-Shabiny, A. M.; Moustafa, A. M.; Ismail, N. S. M.; Pillai, G. G.; Panda, C. S.; Hall, C. D.; Katritzky, A. R. *Org. Biomol. Chem.* **2015**, *13*, 1741.
50. Girgis, A. S.; Saleh, D. O.; George, R. F.; Srour, A. M.; Pillai, G. G.; Panda, C. S.; Katritzky, A. R. *Eur. J. Med. Chem.* **2015**, *89*, 835.
51. CODESSA-Pro Manual, pages 57.